LAPP-EXP-94.05
MARCH 1994

DD

SW 94/15

FIBRE TRACKING

AN OVERVIEW

Jean-Marc Gaillard
L.A.P.P. Annecy

SCIFI 93, October 24-28, 1993
Notre Dame, IN 46456, USA

L.A.P.P. B.P. 110 F-74941 ANNECY-LE-VIEUX CEDEX • TÉLÉPHONE 50.09.16.00 + • TÉLÉCOPIE 50 27 94 95

FIBRE TRACKING: AN OVERVIEW

Jean-Marc Gaillard, LAPP
74941 Annecy le Vieux, France

During the past decade remarkable advances have been achieved in the technology of scintillating plastic fibres and in their utilisation for the construction of tracking detectors.

A pioneer large size fibre tracking detector was built as part of the upgrade of the UA2 central detector[1,2] at the SPS proton-antiproton collider (Fig. 1). The cylindrical fibre detector of average radius 40 cm consisted of 60000 (Ø = 1 mm) plastic fibres with an active length of 2.1 m. One of the main motivations for the upgrade was to improve the electron identification. Thus the fibre detector comprised within 6 cm: 18 tracking layers, a 1.5 Xo tapered lead converter and 6 preshower layers. For space point reconstruction the fibre layers were grouped by stereo triplets with angles 0, $\pm \alpha$, as indicated on Fig. 2. The fibre ends were bunched, as shown, to be coupled to read-out systems of image intensifier plus CCD, 32 in total, similar to those to be used by the Chorus experiment (see below). The quality and the reliability of the UA2 fibre detector performance exceeded expectations throughout its years of operation, paving the way for future fibre detectors. As an illustration of the detector performance, Fig. 3 shows the charge distributions observed in the preshower detector for 40 GeV test beam pions and electrons (Fig. 3a) and for electron candidates from $W \rightarrow e\nu$ (Fig. 3b).

The main properties of the Chorus fibre tracker at CERN will be described in Section 1. Fibre tracker development in the United States centered around the visible light photon counter (VLPC) will be covered in Section 2. As a conclusion to the present overview, a few examples of the use of image intensifiers and of scintillating fibres in biological instrumentation will be described.

Introductory Talk at the Workshop on Scintillating Fibre Detectors,
Octobre 24-28 1993, Notre Dame, IN 46456, USA

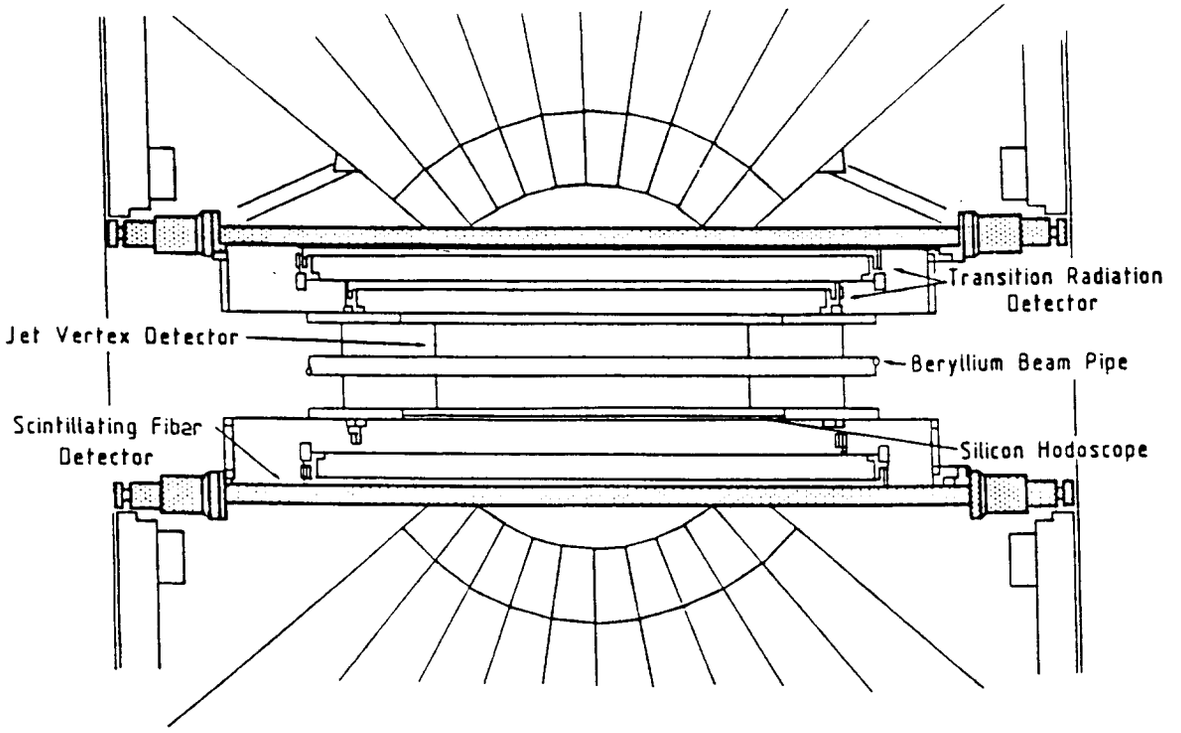

Fig. 1
The Central Detector of the upgraded UA2 apparatus.

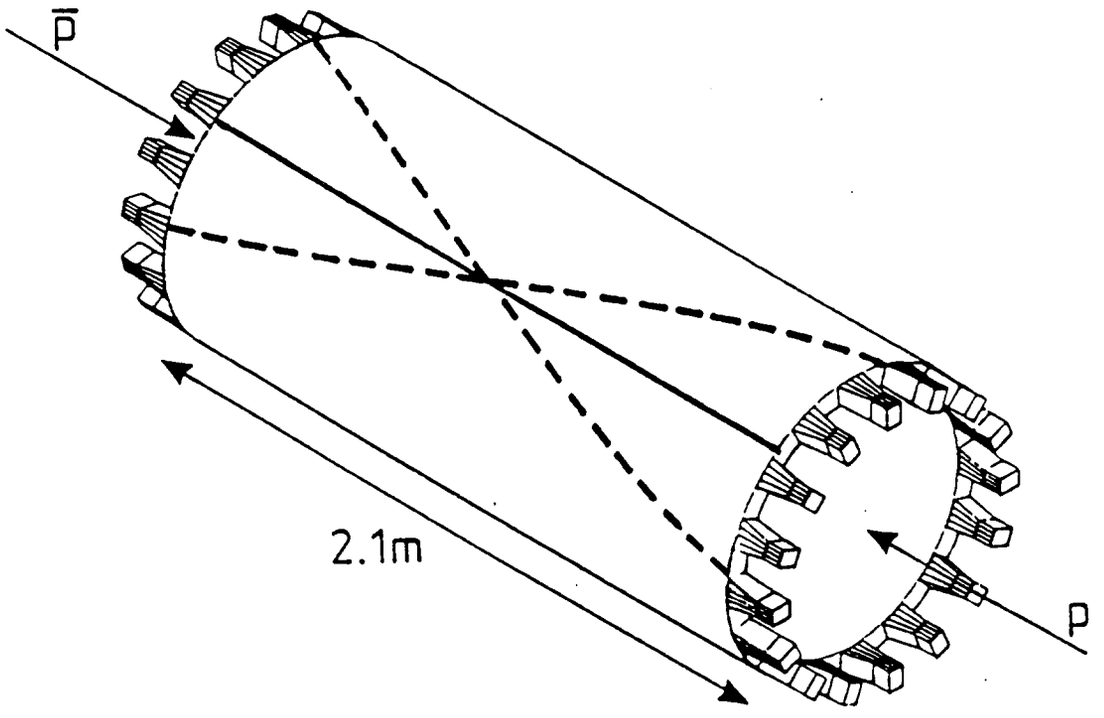

Fig. 2
The geometry of the UA2 Scintillating Fibre Detector. The orientation of the fibre layers and the arrangement of the read out chains are shown.

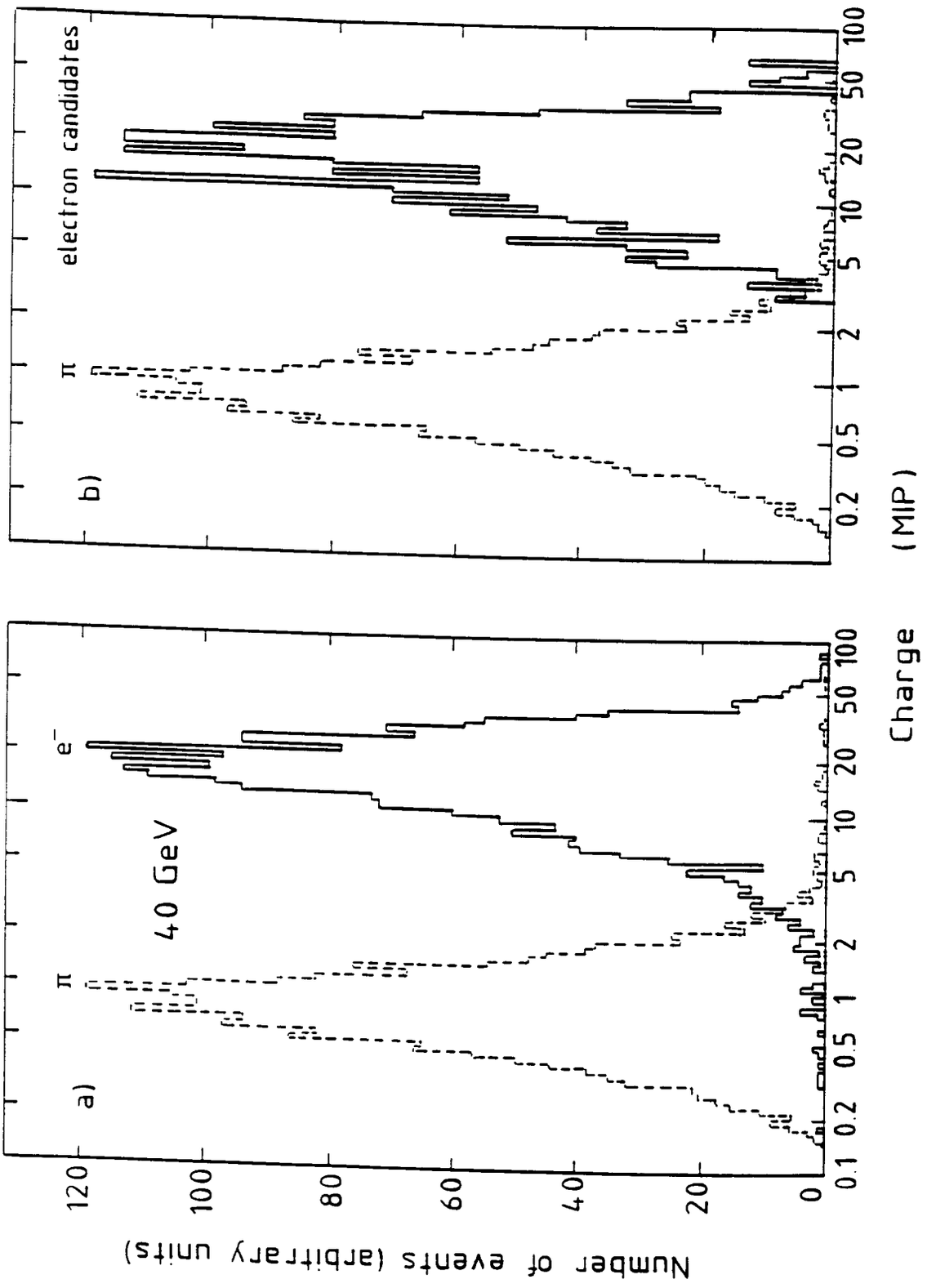

Fig. 3
The pulse height distribution in the UA2 fibre preshower of : a) 40 GeV pions and 40 GeV electrons as measured at a test beam, b) 40 GeV pions, as in a), and electron candidates from the $W \rightarrow ev$ sample.

The main technical features of the Chorus fibre trackers are summarized in Table 1. The number of fibres is almost 20 times that of the UA2 detector. Because their diameter is 0.5 mm instead of 1 mm for UA2, the area of each triangle is 4 times smaller. Like UA2

1. The Chorus Fibre Tracker

In the CERN neutrino beam two experiments, Chorus[3] and Nomad[4], are set up to search for $\nu_\mu \rightarrow \nu_\tau$ oscillation. In the Chorus experiment (Fig. 4) the SPS neutrino beam interacts with a 230 litres (800 kg) emulsion stack made of 2×25 emulsion layers. The experiment will make use of the measurement accuracy in the emulsion to see the track of the short lived τ decay and its decay products. Essential to the success of the experiment is an accurate prelocalisation of the region to be scanned within the emulsion for the neutrino interaction and the τ decay vertex. As shown on Fig. 5 the bulk emulsion targets are followed by scintillating fibre tracking devices which provide a precise prediction of the track impacts on intermediate changeable tracking emulsion plates.

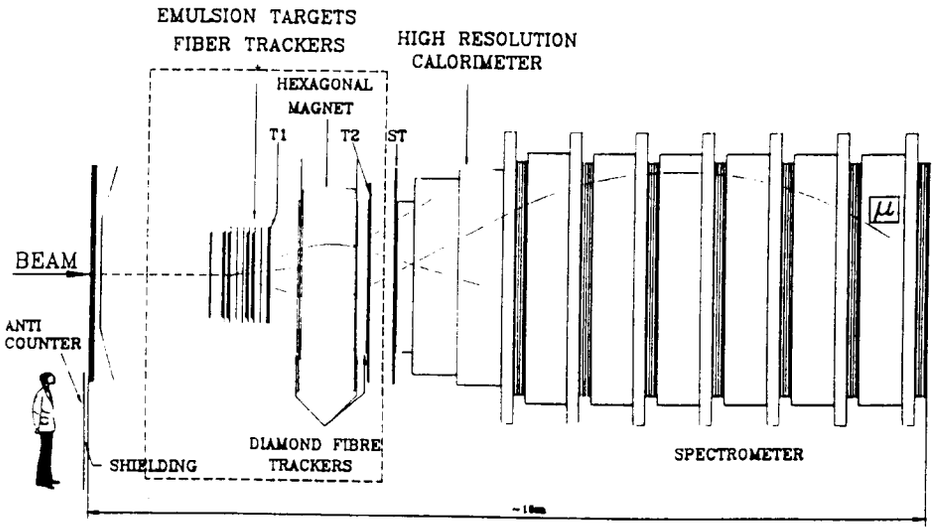

Fig. 4

The apparatus of the Chorus experiment, a search for $\nu_\mu \rightarrow \nu_\tau$ oscillations.

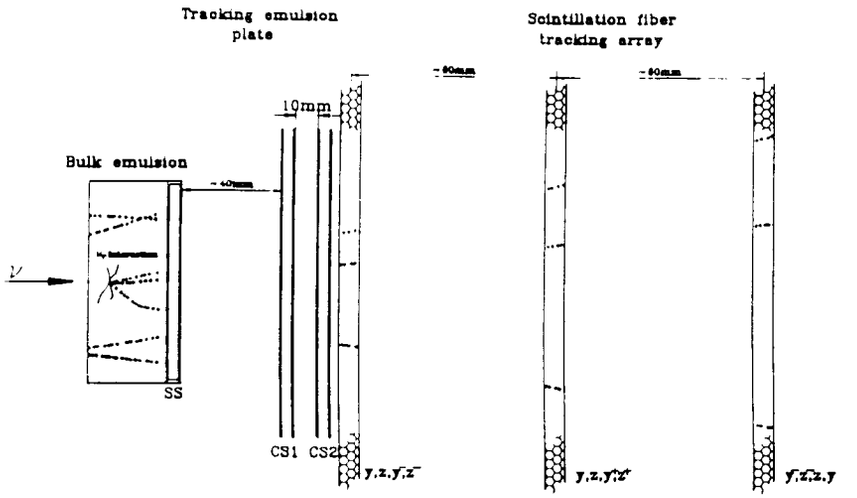

Fig. 5

Tracking in the target region of the Chorus detector.

The main technical features of the Chorus fibre trackers are summarized in Table 1. The number of fibres is almost 20 times that of the UA2 detector. Because their diameter is 0.5 mm instead of 1 mm for UA2, the area of read-out is only 4 times larger. Like UA2, Chorus uses image intensifier chains (Fig. 6) 40 for the target area and 18 for the diamond fibre trackers. The detailed composition of a read-out chain is shown on Fig. 7 : four stages of image intensifiers, with a reduction from an input diameter of 100 mm to an output of 11 mm, coupled to a CCD with 550×288 pixels. The system is equipped with a gate acting on the high gain microchannel plate (MCP) stage. A fast clear (1 μs) can be applied to the CCD to dispose of unwanted events. In addition to its sensitive region, the CCD has a memory region of equal size. Thus, as the neutrino beam intensity is split between two 6 ms spills separated by 2.5 s for each 14.4 s machine cycle, the system has a capacity to collect 2×2 events per accelerator cycle.

Table 1

CHORUS

FIBRE TRACKERS MAIN TECHNICAL FEATURES

	Cross section (cm^2)	Fibre number	Fibre length (km)
Target	1800	720 000	1750
Diamond	800	320 000	750
Total	2600	1 040 000	2500

The Chorus experiment will start to run in the Spring of 1993. Meanwhile the UA2 read-out image intensifier chains, with 95% of their life charge left, are recycled into a heavy ion experiment, WA98, on the SPS at CERN.

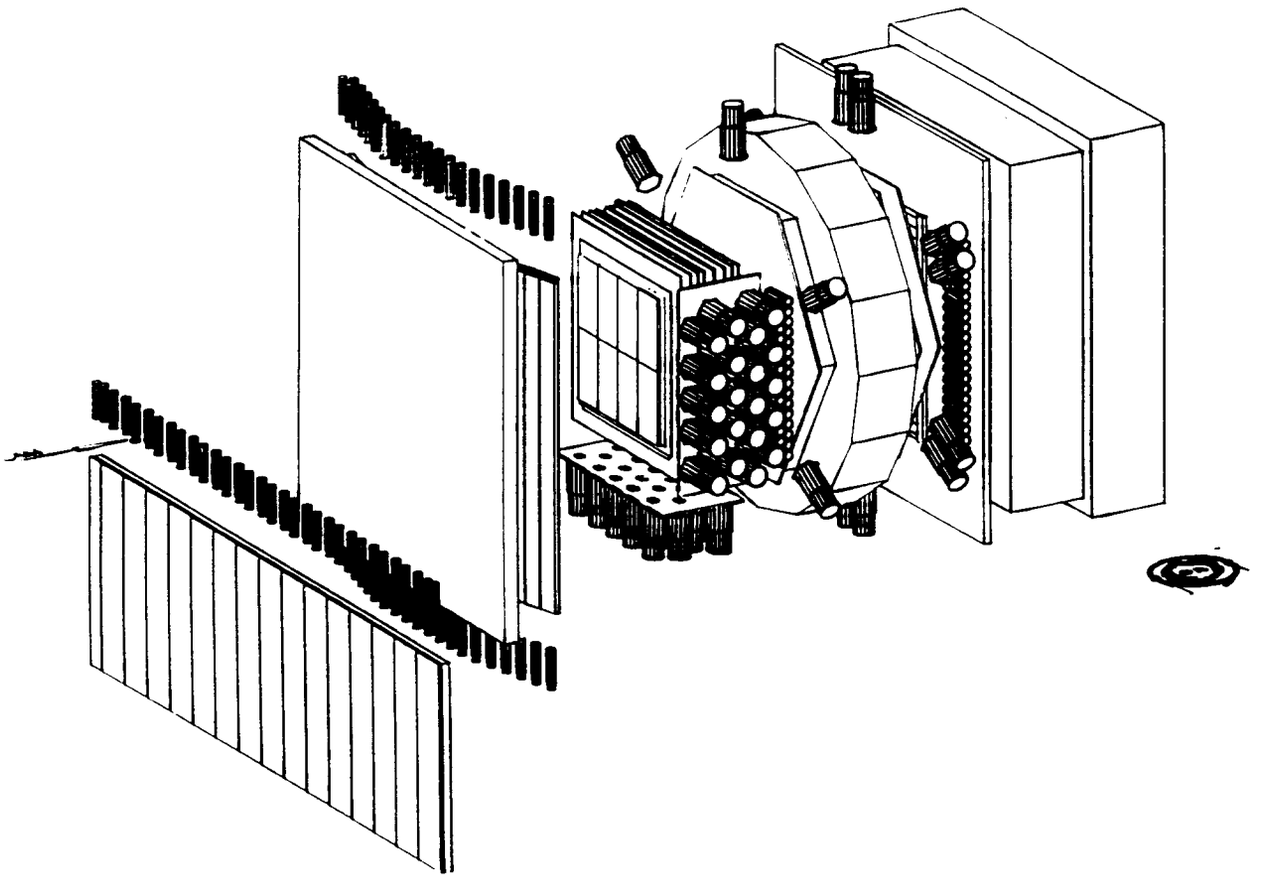

Fig. 6
The Chorus fibre trackers and the distribution of their read-out systems.

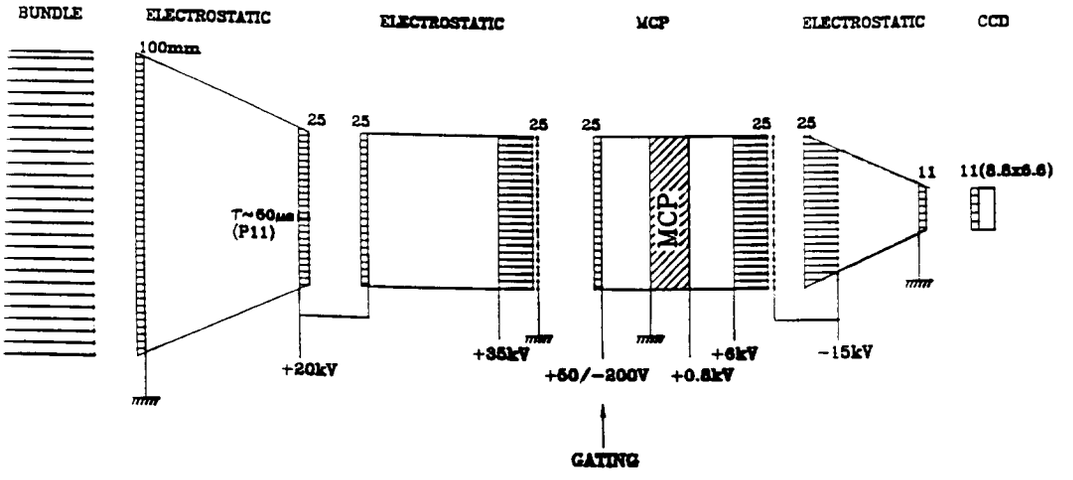

Fig. 7
A chain of four image intensifiers coupled to a CCD for the Chorus tracker read-out.

2. The Visible Light Photon Counter Road

The developments in fibre tracking detectors in the United States have been centered around a new type of read-out device, the Visible Light Photon Counter (VLPC) proposed by M. Atac, which is derived from the Solid State Photomultiplier developped by Rockwell[5]. Some of the properties of the present VLPC'S are given in Fig. 8. The full curve shows the VLPC pulse height spectrum taken with a pulsed light source. The discrepancy from the expected dotted curve at large pulse heights is attributed to an amplifier saturation.

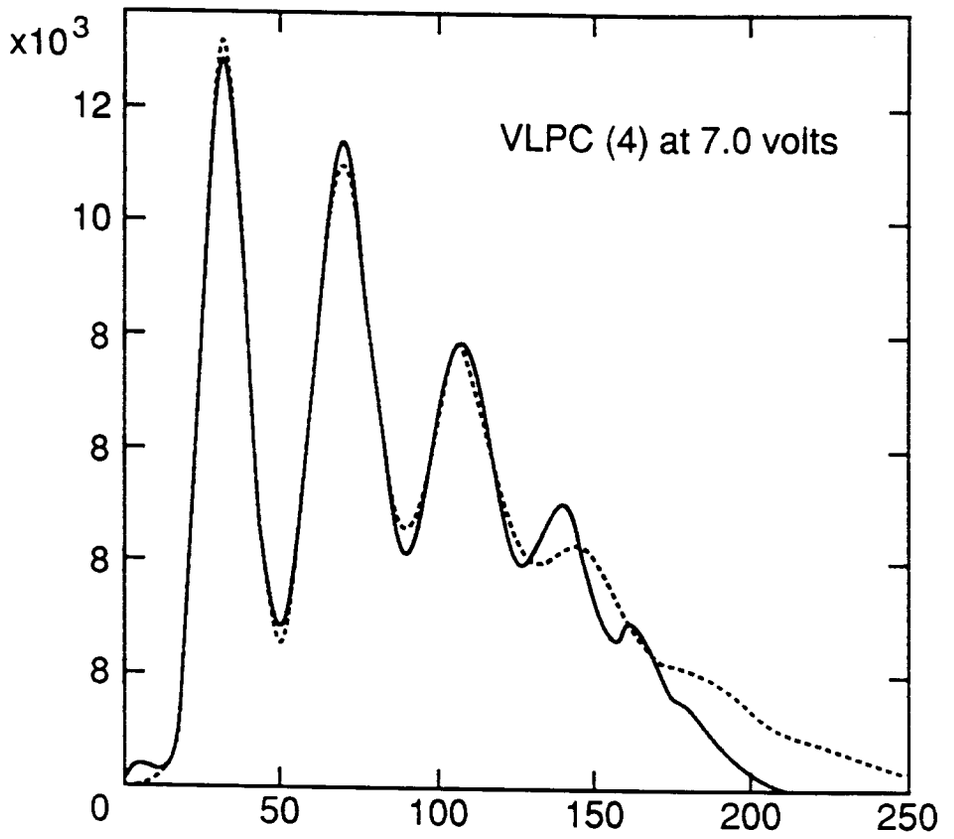

Fig. 8
The pulse height spectrum from a Visible Light Photon Counter
using a pulsed light source as input

The VLPC is a very attractive light detector: fast with 8 ns risetime, excellent quantum efficiency as high as 80%, adequate gain of 20000. It has one main drawback: the need to operate at cryogenic temperatures ~ 7° K. Later during the course of this meeting, industrial participants will describe rather handy cryogenic sets which can handle 2048 channels in 16 removable cassettes. However, since any cryogenic system of VLPC's must be located outside the corresponding complete detector, there are substantial light losses caused by ~ 6 m extra clear fibre length and connectors.

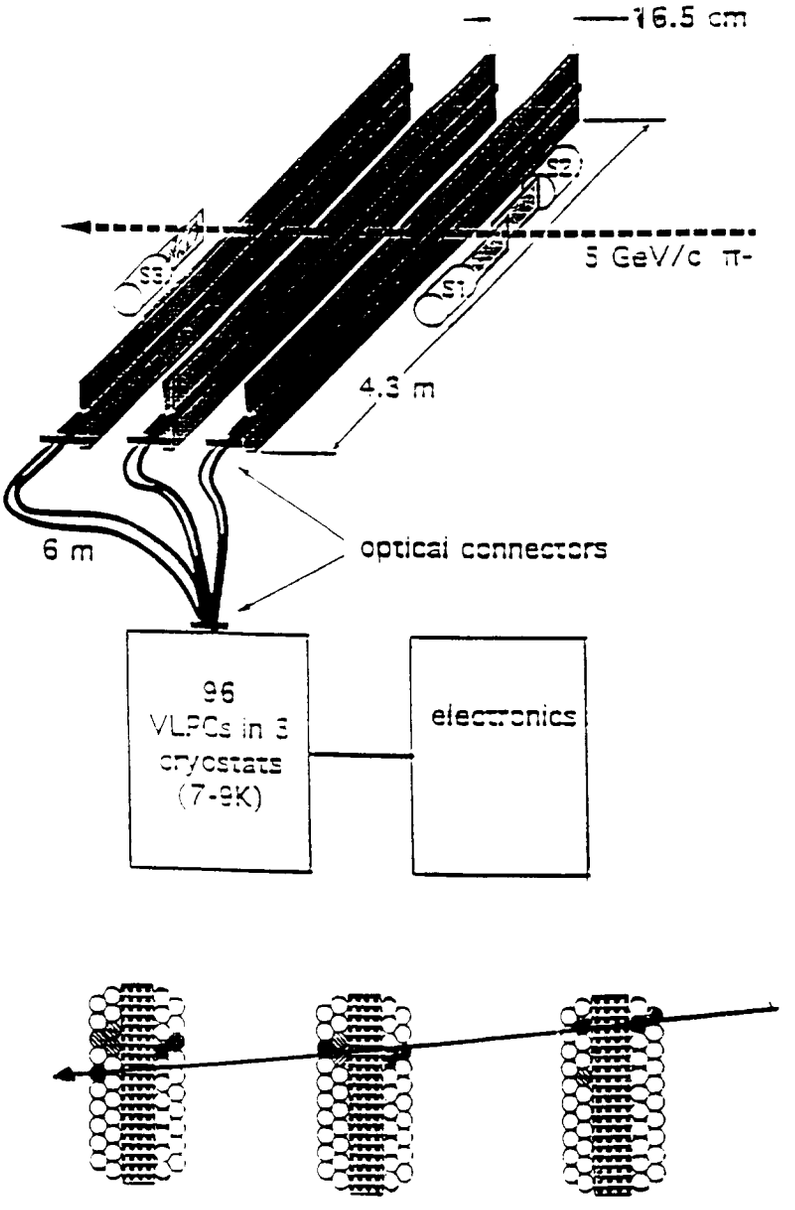

Fig. 9
Beam test of a 12 layer scintillating fibre set up read-out by an array of Visible Light Photon Counters. A typical event is also shown.

The use of fibres and VLPC's was proposed for two tracking detectors: D0 upgrade and SDC. Extensive tests were performed to ascertain the performance of such systems. In particular a 96 - channel, 3 superlayer scintillating - fibre tracking system with VLPC read-out was tested in a 5 GeV/c π^- beam at BNL[6]. The set-up is shown on Fig. 9, together with an event display and a typical reconstructed track. The doublet resolution was measured to be 150 μm with ribbons made of 3 HF fibres 830 μm in diameter. As anticipated the light yield obtained from the farthest end of the fibre was small, 1.2 ± 0.1

photoelectrons.

The need for more photons has led to an interesting multi-clad fibre development (Fig. 10). The fraction of light trapped within a fibre is $(n_{FIBRE}-n_{CLADDING})/n_{FIBRE}$ in each direction along the axis. Lowering the refraction index of the cladding to increase the light yield had been tried over the years with little success due to the lack of adherence between the scintillator and the low index cladding material. The double cladding product shown on Fig. 10b increases the light yield by a factor of 1.7, on average, and is mechanically stable. The comparison between the responses of the single and double cladding fibres shows that increase factor to be constant, within ± 10%, along 12 m of fibre. Due to this and to other improvements, mainly that of the VLPC quantum efficiency which has now reached 80%, the number of photoelectrons would appear to have been fully adequate for a SSC detector.

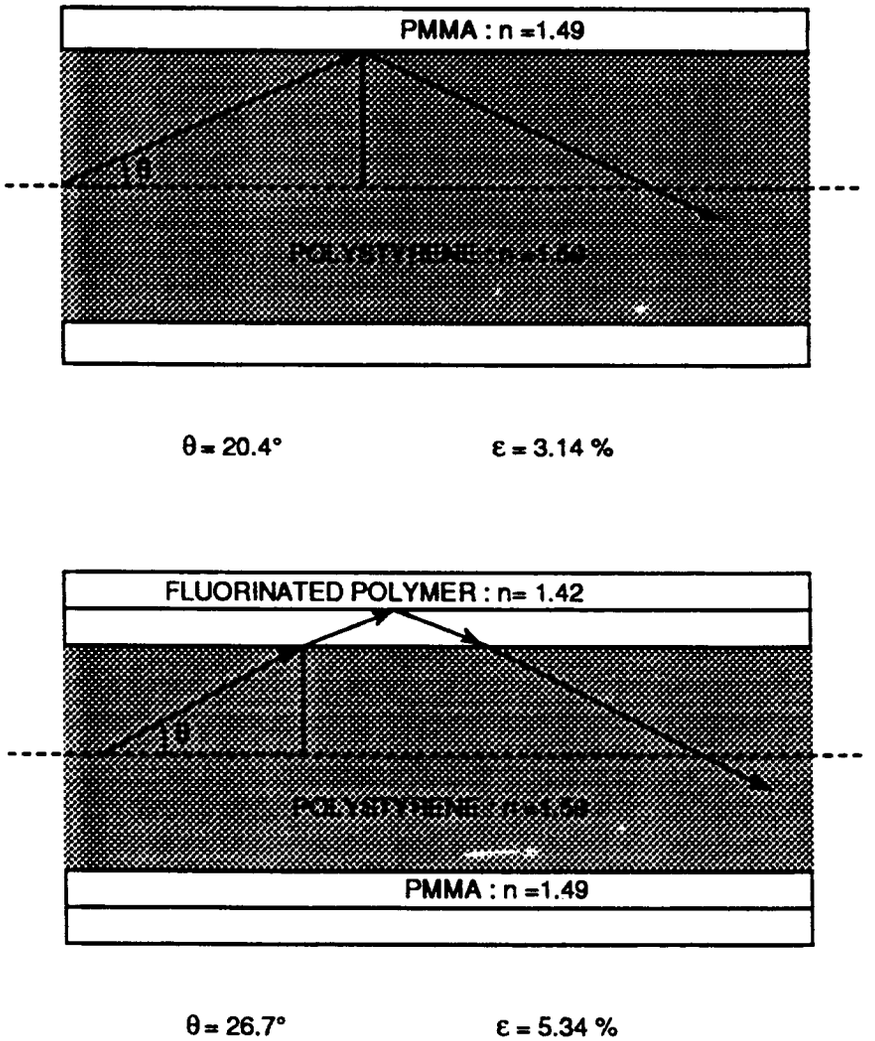

Fig. 10
Single-clad and multi-clad fibres: parameters and properties.

In Table 2, I have collected significant elements of comparison between the fibre tracker of the Chorus experiment and that proposed to the SDC collaboration for SSC. Among all the differences between the two set-ups, those connected to the read-out systems are clearly the most important ones. In my opinion, the future of fibre tracking in particle physics will largely depend upon the ability to promote efficient cost effective read-out.

Table 2

	CHORUS	SFT
FIBRES	10^6	0.5×10^6
LENGTH	2.3 – 2.6	4 + 6m
TYPE	SCSF 38	3 HF
DIAMETER	500 μm	925 μm
END MIRROR	80%	(>50%)
LIGHT	>3pe/mm	λ_{att}=5.2m
CONNECTORS	NO	0.6
MULTICLAD	NO	1.7
READ OUT	58 II	VLPC
EFFICIENCY	16%	70 – 80%

3. Tracking and Biological Instrumentation

A group of physicists from Orsay and Paris[7] are currently developping instrumentation for Biology. As they make use of scintillating fibres and image intensifiers, I was able to offer some contribution to their work and I have experienced much stimulation from the collaboration. As an important refreshing perspective to this overview, I wish to present briefly two examples of biological instruments developped by that group, which are in the course of being commercialized.

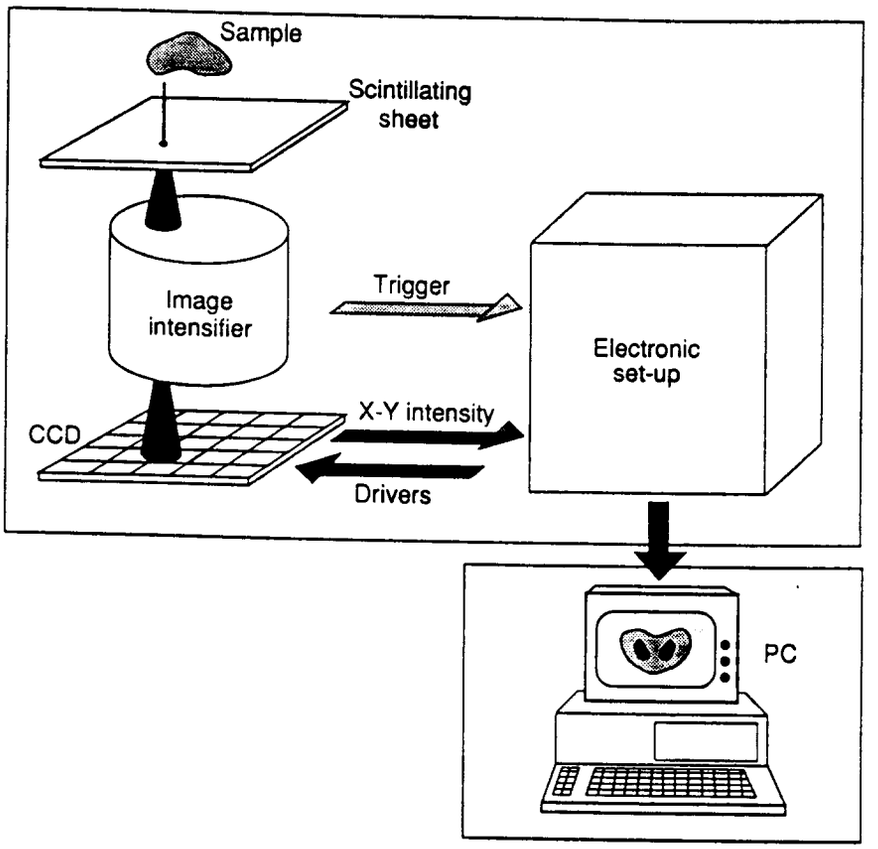

Fig. 11
The High Resolution ß Radio Imager operating principle.

The principle of the High Resolution ß Radio Imager[8] is shown on Fig. 11. It comprises a scintillator sheet above which the radioactive sample to be analysed is positionned and an intensified CCD driven in a single shot mode. Within the proximity focused image intensifier (Fig. 12), the scintillator light is converted into electrons, the electrical signal is then amplified and, finally, it is converted back into a light output in the anode phosphor screen. The light gain is about 10^5. The output is read and processed by a CCD system.

In the initial version of the radio imager, the trigger to the acquisition was provided by a PM placed above the image intensifier on the other side of the sample. Extrapolating from my own experience with the UA2 read-out system, I proposed to develop a self-triggering system[9] by using the prompt electrical pulse which is also present at the anode (Fig. 12). That feature is now available on the commercial device. The Radio Imager has a resolution of 15 μm and a detection efficiency of 60% for a ^{35}S radioactive implant.

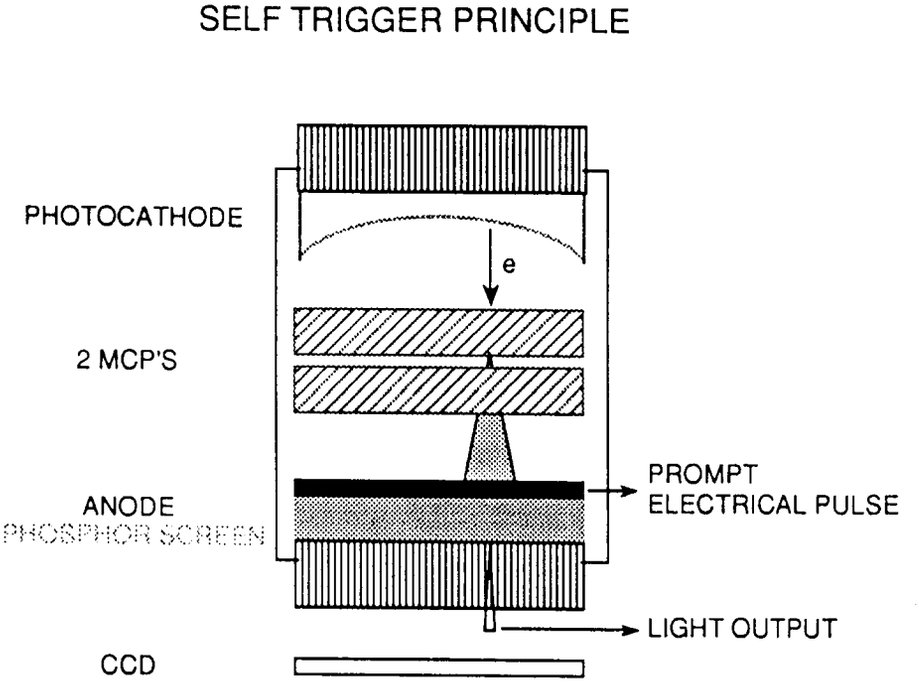

Fig. 12
The self-triggering system of the Radio Imager intensifier.

The radioactive biological samples are obtained by a technique known as "hybridization in situ" whose principle is shown on Fig. 13. The biological tissue to be analysed is first immersed into a solution containing complementary DNA copies labelled with a radioactive element, ^{35}S for the example shown below. The copies couple selectively with the RNA's of the biological tissue. As the copies are largely in excess, they saturate the sample whose measured radioactivity is proportional to the RNA density in the cells: the method is quantitative.

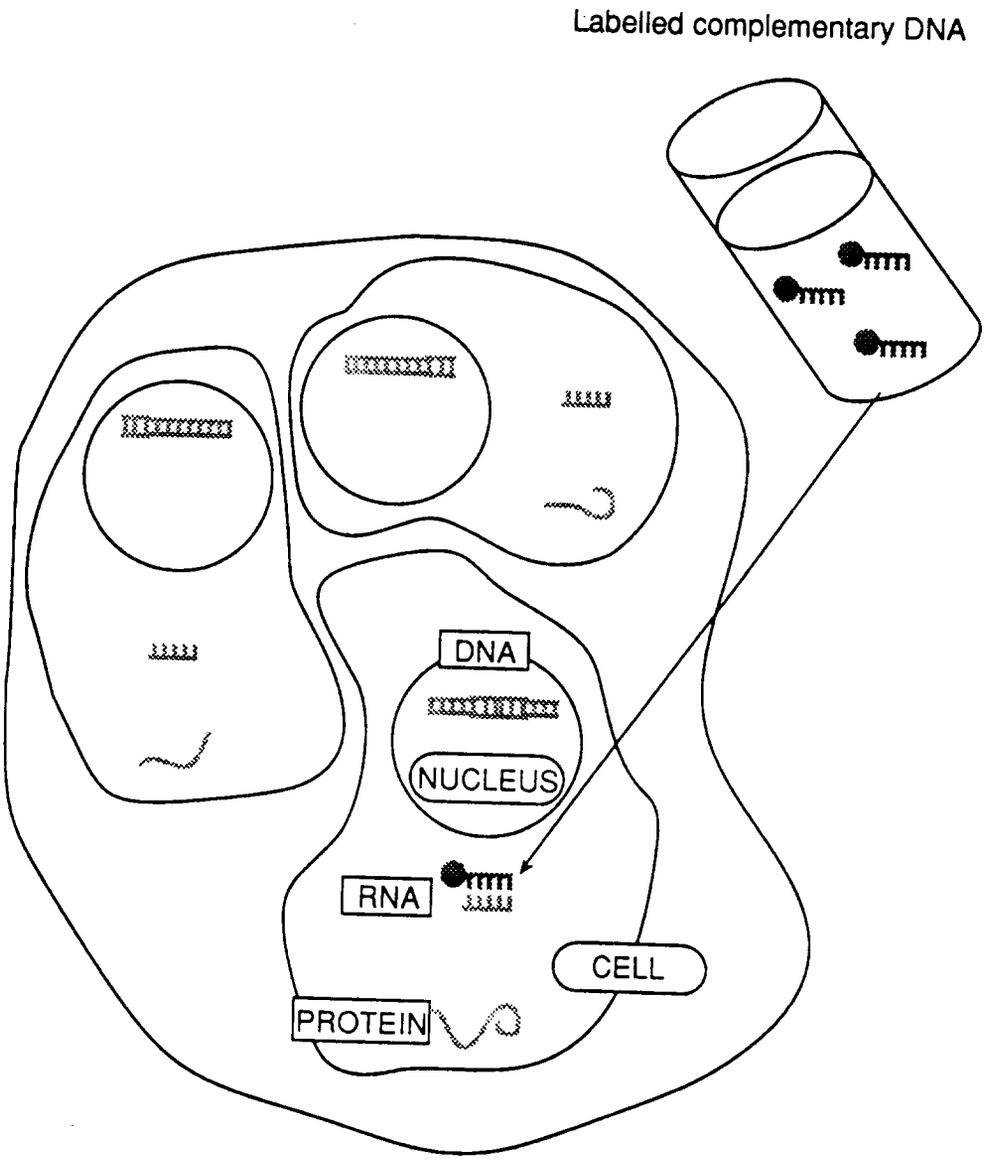

Fig. 13
Principle of the hybridization in situ of a biological sample.

The radio image (0.9 × 1.4 cm^2) shown on Fig. 14 is that of a frontal section of a rat brain, where Neuromodulin-2 (NM2) mRNA, a novel gene whose expression is regulated during the memory process, was detected by in situ hybridization.

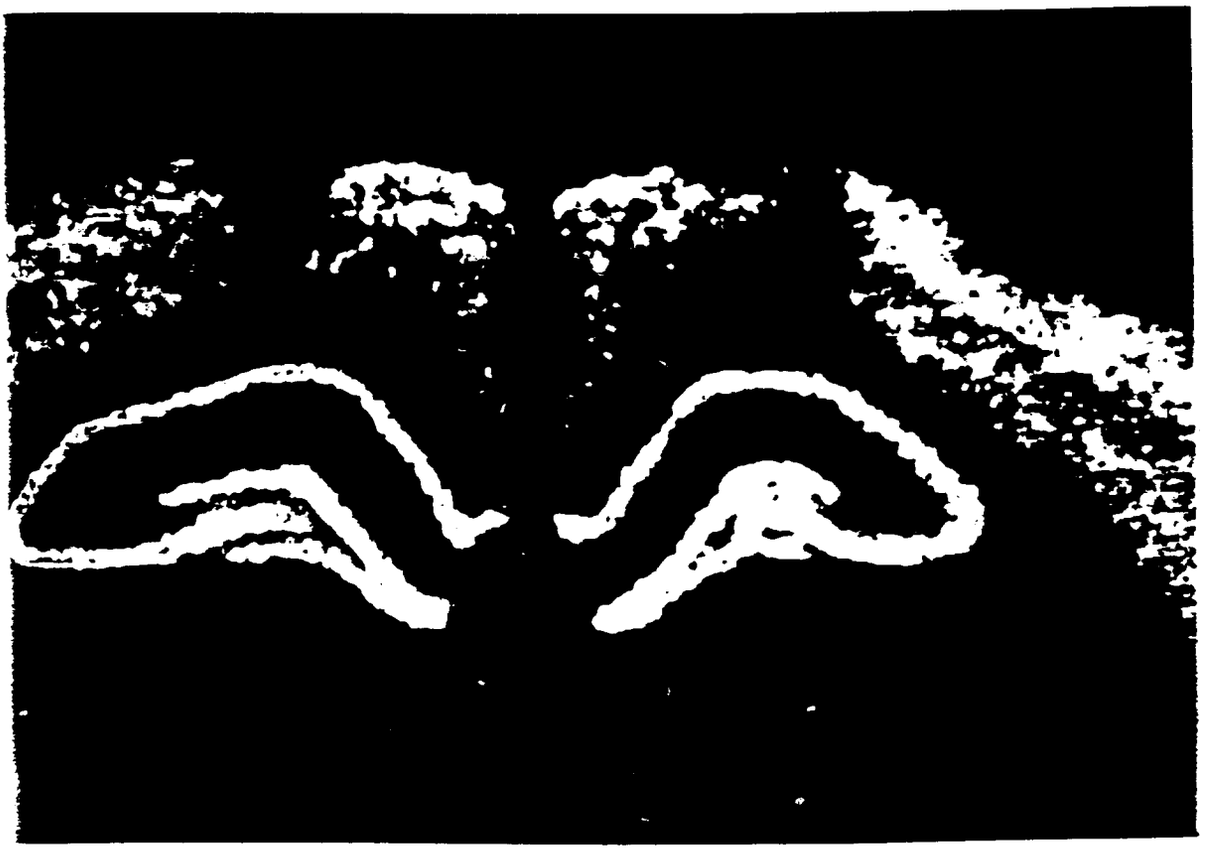

Fig. 14
Expression of neuromodulin-2 (NM2) mRNA in a fontal section of a rat brain.

As shown in the figure, the gene expression is located in the hippocampus, the structure visualized on the lower half of the image, a group of neurons which plays a crucial role in the mechanisms of learning and memory. Indeed, the information is stored in this structure during several weeks until final storage in the cortex (upper part of the image). Thus, in the absence of hippocampus, the memory of the past would be preserved, but no new information could be acquired. The measurements aim at quantifying the gene expression modulations in the hippocampus during the memorization process in order to understand the corresponding role of this gene in the memory mechanisms.

A few properties of the Radio Imager are listed below:

- real time imaging of radioactive samples labelled with ^{14}C, ^{32}P, ^{35}S, ^{125}I, Tritium ...
- spatial resolution 15 μm and detection efficiency 60% for the ß emitter ^{35}S
- image collection duration 10^2 times shorter than with earlier emulsion methods
- up to 30 events acquired per second for a 1.4 × 0.9 cm^2 analysed area.

The Scintillating Optical Fibre Imager (Fig. 15) is another device to measure samples over a much larger analysis area with a coarser resolution. Here the radioactive sample is placed in contact with two orthogonal layers of contiguous Ø = 0.5 mm scintillating fibres. Electrons emitted by the sample cross the fibres from both layers producing light which is read-out from both fibre ends by a multianode photomultiplier (PMMA). The use of different fibre combinations at each end in order to register and code the information allows the system to separate 2 × 512 fibres with only 2 × 32 channels. This imager is used in experiments of molecular biology. It is much more powerful than earlier X-ray instrumentation.

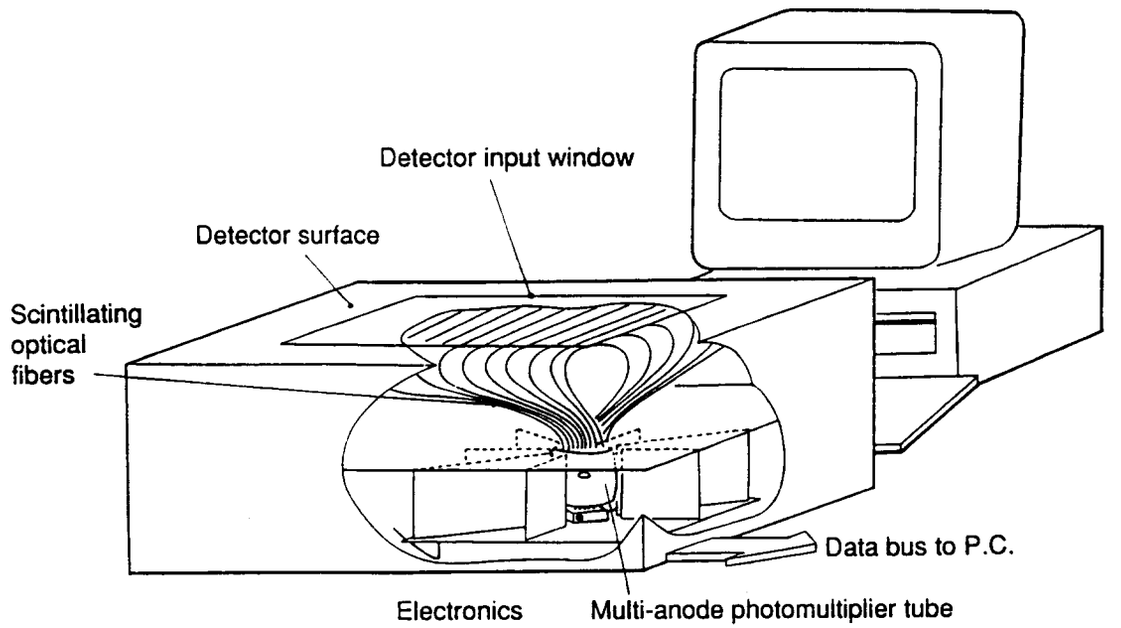

Fig. 15
The Scintillating Optical Fibre Imager with a detection area of 12.8 × 12.8 cm^2, as shown, or larger.

The fibre and the radio imagers have a wide range of applications which are not restricted to biology. For example, both types of imagers have been used recently[11] to study ^{223}Ra migration in sandstone core samples from a surface site radioactive waste disposal (Manche Site). To conclude, after several years of struggle for recognition, a new interdiscipline has emerged with great hopes for the future.

* * * * *

As this is only an overview, I will end here by wishing a scintillating future for the fibre tracking during this meeting and for the detectors to come.

REFERENCES

1. Proposal to improve the Performance of the UA2 Central Detector CERN/SPSC 84-95 (1984).

2. J. Alitti et al., Nucl. Instr. and Meth. A279 (1989) 364.

3. CHORUS Collaboration, CERN-SPSC/90-42 and CERN-PPE/93-131.

4. NOMAD Collaboration, CERN-SPSLC/91-21 and CERN-SPSLC/92-51.

5. M.D. Petroff, M.G. Stapelbroek and W.A. Kleinhans, Appl. Phys. Lett. 51 (1987) 406;
   M.D. Petroff and M.G. Stapelbroek, IEEE Trans. Nucl. Sci. NS-36 (1989) 158;
   M.D. Petroff and M. Atac, ibid, p. 163.

6. Beam Test of a 12-layer Scintillating-Fibre Charged-Particle Tracking System, B. Abbott et al., Preprint PU-93-676 (Purdue University), submitted to Nucl. Inst. and Meth. A.

7. L. Valentin Research Group. Institut de Physique Nucléaire, 91406 Orsay Cedex, France. Laboratoire de Physique Nucléaire Paris 7, 75251 Paris Cedex 05.

8. Y. Charon et al., Nucl. Instr. and Meth. A292 (1990) 179.

9. Y. Charon et al., Nucl. Instr. and Meth. A310 (1991) 379.

10. R. Mastrippolito et al., Biotechnics, Vol. 11, n° 6 (1991) 778.

11. Y. Charon et al., Radiochimica Acta 58/59 (1992) 205.